

# Tristhiolato Pseudopeptides Bind Arsenic(III) in an AsS<sub>3</sub> Coordination Environment Imitating Metalloid Binding Sites in Proteins

Levente I. Szekeres, Pascale Maldivi, Colette Lebrun, Christelle Gateau, Edit Mesterházy, Pascale Delange,\* and Attila Jancsó\*



Cite This: *Inorg. Chem.* 2023, 62, 6817–6824



Read Online

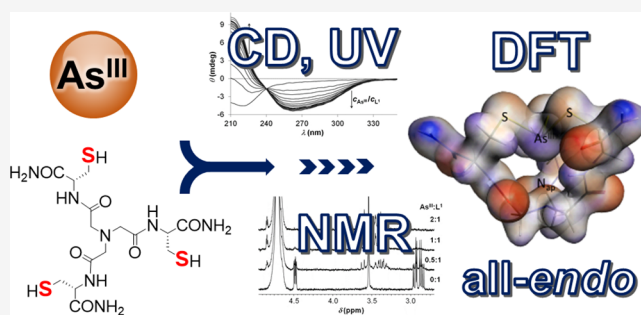
ACCESS |

Metrics & More

Article Recommendations

Supporting Information

**ABSTRACT:** The As<sup>III</sup> binding of two NTA-based tripodal pseudopeptides, possessing three cysteine (ligand L<sup>1</sup>) or D-penicillamine residues (ligand L<sup>2</sup>) as potential coordinating groups for soft semimetals or metal ions, was studied by experimental (UV, CD, NMR, and ESI-MS) and theoretical (DFT) methods. All of the experimental data, obtained with the variation of the As<sup>III</sup>:ligand concentration ratios or pH values in some instances, evidence the exclusive formation of species with an AsS<sub>3</sub>-type coordination mode. The UV-monitored titration of the ligands with arsenous acid at pH = 7.0 provided an absorbance data set that allowed for the determination of apparent stability constants of the forming species. The obtained stabilities (logK' = 5.26 (AsL<sup>1</sup>) and logK' = 3.04 (AsL<sup>2</sup>)) reflect high affinities, especially for the sterically less restricted cysteine derivative. DFT calculated structures correlate well with the spectroscopic results and, in line with the <sup>1</sup>H NMR data, indicate a preference for the all-*endo* conformers resembling the As<sup>III</sup> environment at the semimetal binding sites in various metalloproteins.



## INTRODUCTION

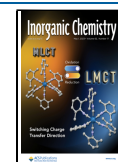
Tristhiolato coordination sites are very important in metalloreulation or detoxification in biology, for instance, for soft metal ions, such as Hg<sup>II</sup> in the regulatory proteins MerR<sup>1</sup> or Cu<sup>I</sup> when trapped in metallothioneins.<sup>2</sup> Interestingly, MS<sub>3</sub> sites are also widely found in arsenic-binding proteins.<sup>3–6</sup> For As<sup>III</sup>, a metalloid with a lone electron pair, a wide range of interactions may dictate the structure of the coordination site. Indeed, the As<sup>III</sup>S<sub>3</sub> center may be in an *endo*- or *exo*-type coordination,<sup>7</sup> *endo* and *exo* referring to the relative orientation of the carbon atoms of the alpha methylene groups and As<sup>III</sup> as compared to the S<sub>3</sub> plane (same side, *endo*; opposite side, *exo*). Repulsive forces between the sulfur lone pairs,<sup>7</sup> steric hindrance due to close proximity of bulky hydrophobic groups around the As<sup>III</sup> lone pair,<sup>7</sup> and secondary bonding interactions between As<sup>III</sup> and various heteroatoms<sup>8–10</sup> or  $\pi$ -systems<sup>9–13</sup> or  $\sigma$ -hole bonding<sup>14,15</sup> may all affect the stability and structure of As<sup>III</sup> complexes.

In this paper, we show that simple bioinspired pseudopeptides, offering a tristhiolato coordination site, induce an AsS<sub>3</sub> coordination only. The two ligands L<sup>1</sup> (NTA(Cys-NH<sub>2</sub>)<sub>3</sub>) and L<sup>2</sup> (NTA(D-Pen-NH<sub>2</sub>)<sub>3</sub>), shown in Scheme 1, were chosen to mimic the AsS<sub>3</sub> coordination found in some biological As<sup>III</sup> binding sites, thanks to a nitrilotriacetic acid anchor grafted with either three cysteine or D-penicillamine moieties. The two ligands display three thiol functions in a tripodal architecture

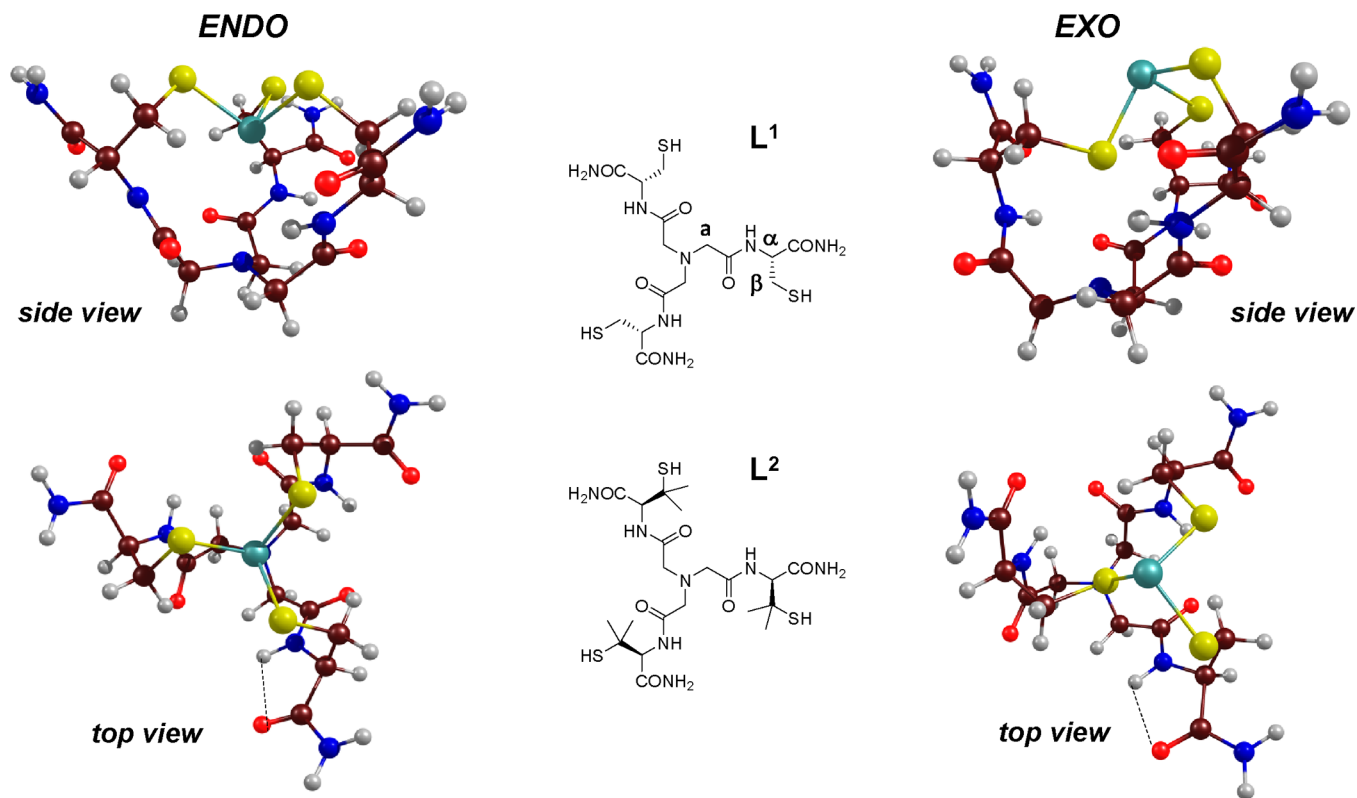
and are prone to offer a tristhiolato coordination site to soft metal ions. A C-terminal neutral primary amide instead of an acid was preferred for the three amino acids to avoid interferences for metal coordination and also electrostatic repulsions in the final complexes at physiological pH. These two sulfur ligands were previously demonstrated to promote a MS<sub>3</sub> coordination with Hg<sup>II</sup> and Cu<sup>I</sup> in aqueous solution buffered at pH 7.4.<sup>16–19</sup> Therefore, we anticipated that L<sup>1</sup> and L<sup>2</sup> could be of interest to model As<sup>III</sup> binding in an AsS<sub>3</sub> coordination. By contrast to Hg<sup>II</sup> and Cu<sup>I</sup>, which are soft metal cations with a 5d<sup>10</sup> and 3d<sup>10</sup> electronic configuration, respectively, As<sup>III</sup> is a metalloid having a 3d<sup>10</sup>4s<sup>2</sup> electronic configuration with the presence of a lone pair that may strongly influence its coordination, as described above. In this work, a detailed analysis of the intimate As<sup>III</sup> coordination sphere in the two As<sup>III</sup>L<sup>1</sup> and As<sup>III</sup>L<sup>2</sup> biomimetic complexes was performed with various experimental data, which were confronted to density functional theory (DFT) calculation.

**Received:** February 18, 2023

**Published:** April 18, 2023



**Scheme 1. Schematic Structure of the Ligands NTA(Cys-NH<sub>2</sub>)<sub>3</sub> (L<sup>1</sup>) and NTA(D-Pen-NH<sub>2</sub>)<sub>3</sub> (L<sup>2</sup>) (Middle) with Notations of the Hydrogens of L<sup>1</sup> Monitored by <sup>1</sup>H NMR Spectroscopy and the B3LYP-D3/def2-tzvp Optimized Structures of the Energetically Favored *endo,endo,endo* Conformer (Left) and the Less Favored *endo,endo,exo* Conformer (Right) of the AsL<sup>1</sup> Species in Side and Top Views<sup>a</sup>**



<sup>a</sup>Color code: arsenic, turquoise; sulfur, yellow; oxygen, red; nitrogen, blue; carbon, brown; hydrogen, white.

This revealed a unique AsS<sub>3</sub> binding site with a structure reminiscent of sites found in As<sup>III</sup>-binding proteins.

## EXPERIMENTAL SECTION

**Materials.** The studied ligands were synthesized and purified, as described before.<sup>16,17</sup> All other chemicals, purchased from Sigma-Aldrich (Merck), were of analytical grade and used without further purification. (Caution: The solid compound arsenic(III) oxide is a chemical with high health hazards (acute toxicity, skin corrosion, serious eye damage, and carcinogenicity) and environmental hazards (long-term (chronic) aquatic hazard) and should be handled with extreme care using the necessary protective equipment. Any solution samples containing the aqueous forms of arsenic(III) are also toxic and must be handled/disposed according to the regulations for toxic liquid wastes.) Aqueous solutions were prepared by using Milli-Q water of ultrapure laboratory grade.

**Preparation of Stock Solutions and Samples for Spectroscopic Studies.** Stock solutions of the ligands were prepared in an oxygen-free argon atmosphere in a glovebox every second day or before a new series of experiments. The solid compounds were dissolved in the buffer solution/solvent used for the specific experiment. The medium of a typical sample was phosphate buffer (20 mM, pH = 7.0). The ionic strength of the samples was adjusted to 0.1 M by NaCl. The concentrations of the stock solutions of the ligands varied between  $5.0 \times 10^{-5}$  and  $1.3 \times 10^{-4}$  M and were determined by Ellman's procedure. According to the procedure, 5,5'-dithiobis(2-nitrobenzoic acid) (DTNB) reacts with the free thiol groups of the ligands and produces a 2-nitro-5-thiobenzoate anion (TNB<sup>2-</sup>) per each reacting thiol group that is detected at 412 nm ( $\epsilon = 14\,150 \text{ M}^{-1} \text{ cm}^{-1}$ ).<sup>20,21</sup> Stock solutions of arsenous acid were prepared weakly by dissolving a precisely weighed mass of arsenic(III)

oxide in a 0.1 M NaOH solution (ca. 2–2.5 mg of As<sub>2</sub>O<sub>3</sub> per 1.0 mL) with heavy stirring under an argon atmosphere (glovebox). The alkaline solution was neutralized by a 1.0 M HCl solution to a pH value between pH ~4 and 6. The final concentration of arsenous acid was adjusted to  $1.0 \times 10^{-2}$  M by adding the necessary volume of Milli-Q water. Samples were prepared by mixing stock solutions of the ligands and arsenous acid.

**Recording UV–Vis Absorption and Circular Dichroism (CD) Spectra.** The UV–vis absorption spectra were measured by using optical fibers connecting an external cell holder, placed in the glovebox, with a Varian Cary 50 spectrophotometer (operating outside the glovebox). The spectra were recorded in a quartz cuvette of a 1.0 cm path length in the wavelength range of 220–550 nm. The baseline was recorded for the empty cell holder and the spectrum of the cuvette, filled with the buffer/solvent used for the preparation of the relevant samples, was subtracted from the spectra of the samples. Data from the wavelength range of 240–335 nm was used for calculating stability constants for As<sup>III</sup> binding by L<sup>1</sup> and L<sup>2</sup> (vide infra). The typical concentrations of the ligands were  $4.1\text{--}5.0 \times 10^{-5}$  M (L<sup>1</sup>) and  $1.0 \times 10^{-4}$  M (L<sup>2</sup>). Aliquots of arsenous acid stock solutions (or base in pH titrations) were gradually added to the ligand solutions and the spectra were acquired after a ca. 10 min waiting time allowing for equilibration. The CD spectra were measured with an Applied Photophysics Chirascan photometer. The instrument was calibrated by using (1S)-(+)-10-camphorsulfonic acid as a reference compound. Data were collected in the wavelength range of 350–190 nm with 1 nm bandwidth and 2 s dwell time per data point. Three scans were measured for each sample, including the background buffer solution. The average spectrum of the scans was corrected by the spectrum of the background and smoothed by the Savitzky–Golay method with a “window size” of 7. Each sample and each addition of the arsenous acid solution of a titration series was performed in the

glovebox under an argon atmosphere in a quartz cuvette, equipped with a Teflon cap. The CD instrument was operated outside the glovebox. The titration protocols were similar to those applied for the UV-vis studies. The concentrations of the ligands were  $2.5 \times 10^{-5}$  M ( $L^1$ ) and  $1.0 \times 10^{-4}$  M ( $L^2$ ).

**Recording ESI-MS Spectra.** ESI-MS experiments were performed on a Thermo Scientific LXQ-linear ion trap instrument equipped with an electrospray ion source. The full scan spectra were acquired in the range of  $m/z = 50$ –1500 or 50–2000 amu in the positive ion polarity mode ( $L^2$  samples) and in the positive and negative ion polarity modes ( $L^1$  samples) by infusion through a fused silica tubing at a flow rate of 2–10 mL min<sup>-1</sup>. The instrument calibration ( $m/z = 50$ –1500) was achieved by following the standard calibration procedure from Thermo Scientific (using a mixture of caffeine, MRFA, and Ultramark 1621). The heated capillary for the LXQ was set in the temperature range of 200–250 °C, while the ion-spray voltage was adjusted in the range of 3–6 kV. The injection time varied between 5 and 200 ms. Samples of  $L^1$  and  $L^2$  were prepared in ammonium acetate buffer (20 mM, pH = 6.9) with ligand concentrations of 100  $\mu$ M. Aliquots of arsenous acid solutions were added to set the desired As<sup>III</sup>: $L^1$  (or  $L^2$ ) concentration ratio.

**<sup>1</sup>H NMR Experiments.** NMR measurements were carried out on a Bruker Avance 400 MHz spectrometer operated at 400.13 MHz (for <sup>1</sup>H). The 1D <sup>1</sup>H NMR spectra were recorded with a spectral width of 10 ppm and a 32,000 time domain by using 64 scans. Samples were prepared in a phosphate buffer in D<sub>2</sub>O ( $c_{\text{buffer}} = 20.0$  mM, pD = 7.21) using  $L^1$  in a concentration of  $c = 90$ –100  $\mu$ M. As<sup>III</sup> was added to the samples of  $L^1$  from a stock solution of arsenous acid prepared in D<sub>2</sub>O by using NaOD for the dissolution of As<sub>2</sub>O<sub>3</sub> and DCl for pD adjustment. To gain a clearer insight on the coordination mode of the As<sup>III</sup>-bound  $L^1$ , a <sup>1</sup>H–<sup>1</sup>H gCOSY experiment, using the *cosygppp*af pulse program, was also carried out in an As<sup>III</sup>: $L^1$  1:1 sample. The 2D spectrum was acquired with 2048(F2) and 256(F1) complex points each in a spectral width of 3.5 ppm applying 280 scans. All spectra were processed by the Topspin 4.0.7 software (Bruker).

**DFT Calculations and Computational Details of Simulating UV and CD Spectra and <sup>1</sup>H NMR Chemical Shifts.** DFT calculations were run with Orca 5.0.<sup>22–24</sup> Geometry optimizations were carried out with the B3LYP hybrid functional including dispersion terms through the D3BJ correction. We checked that numerical frequencies were all real for the optimized geometries presented here. The solvent was taken into account using a polarizable continuum model (cpcm) for water. The all-electron def2-tzvp basis set was used for all atoms. Default integration and grid accuracy parameters were used, together with a TightSCF criterion. Starting geometries were built with a C3 geometry first with *endo,endo,endo* geometries and both possible helices (clockwise and anticlockwise). Optimization slightly distorted the trigonal symmetry for these all-*endo* structures as revealed by bond lengths, even with tight convergence criteria. From the C3 starting geometry, the *exo* ones were generated by moving the As atom outside the cavity along the C3 axis to generate an *exo,exo,exo* position. But the latter relaxed always to an *exo,endo,endo* conformation; thus, it loses the trigonal symmetry. Simulations of the UV and CD spectra were based on TDDFT approaches with 30 excitations in a continuum model for solvation in water, with B3LYP and def2-tzvp basis sets. <sup>1</sup>H NMR chemical shifts were obtained by calculating the shielding tensor within the gauge-including atomic orbital (GIAO) origin and using the TMS proton shielding tensor as the reference. The TPSS functional with pcSeg-2 basis set was chosen based on previous works.<sup>25</sup> Building and displaying structures and spectra were done using Chemcraft.<sup>26</sup> Electrostatic potential visualization was done with the AMS GUI package<sup>27</sup> on single points with ADF 2016 (B3LYP and TZ2P basis sets) using the previously optimized geometries.

**Calculation of the As<sup>III</sup> Binding Affinities of the Ligands.** The spectra of the As<sup>III</sup> titration series of  $L^1$  and  $L^2$  were evaluated by the PSEQUAD software<sup>28</sup> using absorbance values from the wavelength range of 240–335 nm. The fitting procedure provided conditional stability constant ( $\log K'$ ) for the AsL species, formed via the  $\text{As} + L \rightleftharpoons \text{AsL}$  equilibrium process at pH = 7.0, characterized by the equation

$K' = [\text{AsL}]/([\text{As}] \times [L])$ . In these formulae, As stands for the free arsenous acid, while L represents the non-coordinated ligand ( $L^1$  or  $L^2$ ) irrespectively of their protonation states. Similarly, AsL is a general notion of the mono-complex adduct irrespectively of the form of the bound components. The molar absorption spectrum of the AsL mono-complex was also an output of the data evaluation process, while the molar absorption spectra of the free ligands at pH = 7.0 were calculated from the first spectra of the As<sup>III</sup> titration series and used as a fixed set of parameters in the fitting procedure.

## RESULTS AND DISCUSSION

Arsenic(III) binding by NTA-based tripodal scaffolds, displaying three thiol groups from cysteine (NTA(Cys-NH<sub>2</sub>)<sub>3</sub> ( $L^1$ )) or D-penicillamine (NTA(D-Pen-NH<sub>2</sub>)<sub>3</sub> ( $L^2$ )) arms (Scheme 1), was studied by a combination of UV-vis, CD, <sup>1</sup>H NMR, and ESI-MS techniques, as well as by geometry optimization using DFT calculations.

**UV-Vis and CD Spectroscopic Studies.** UV-vis-monitored titrations of  $L^1$  at pH = 7.0 by solutions of arsenous acid reflect a monotonic absorbance increase between 220 and 350 nm, as a function of the As<sup>III</sup>: $L^1$  concentration ratio, leveling off only at a few-fold As<sup>III</sup> excess over the ligand (Figure 1). The recorded spectra display a shoulder-like feature

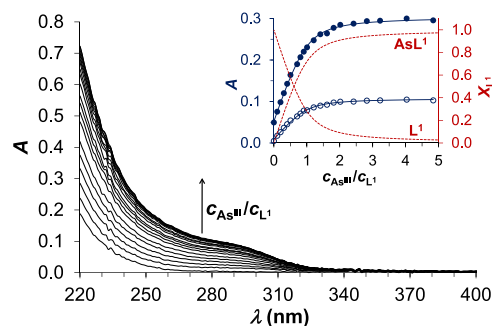


**Figure 1.** UV spectra of  $L^1$  recorded in a titration with arsenous acid (As<sup>III</sup>) at pH = 7.0 ( $c_{L^1} = 50$   $\mu$ M in phosphate buffer, 20 mM,  $I = 0.1$  M NaCl). The inset shows the measured (shaded circle, 240 nm; unshaded circle, 280 nm) and fitted (continuous blue lines, left axis) absorbances as well as the relative fractions of the free and bound ligand (red dashed lines, right axis) as a function of the  $c_{\text{As}^{\text{III}}}/c_{L^1}$  concentration ratio.

between 270 and 300 nm, very similar to that observed in the UV-vis spectra of As<sup>III</sup>-glutathione (GSH)<sup>29,30</sup> and, with a less characteristic shoulder-shape, in the systems of dihydrolipoic acid (DHLA),<sup>30</sup> dimercaptosuccinic acid (DMSA),<sup>30</sup> or 2,3-dimercaptopropan-1-ol (BAL)<sup>31</sup> under conditions where the coordination of three sulfur donors to As<sup>III</sup> has been suggested. The same type of band, assigned to  $S^- \rightarrow \text{As}^{\text{III}}$  ligand-to-metal charge transfer transitions (LMCT),<sup>29,30,32–34</sup> seems to occur at slightly higher energies (250–270 nm) when only two thiolates are bound to the As<sup>III</sup> center, as exemplified by data for dithioerythritol (DTE)<sup>32</sup> and dithiothreitol (DTT).<sup>30</sup> The molar absorption coefficient calculated for the proposed AsL<sup>1</sup> complex (see below) is  $\epsilon_{280\text{nm}} = 2.2 \times 10^3 \text{ M}^{-1} \text{ cm}^{-1}$ , which is rather similar to what was reported for the As(GSH)<sub>3</sub> complex,<sup>29</sup> and significantly larger than the estimated values in species with two As<sup>III</sup>-thiolate bonds ( $\epsilon_{280\text{nm}} \sim 4.8$ – $6.4 \times 10^2 \text{ M}^{-1} \text{ cm}^{-1}$ ;  $\epsilon_{260-270\text{nm}} \sim 0.85$ – $1.0 \times 10^3 \text{ M}^{-1} \text{ cm}^{-1}$ ).<sup>30–32</sup> The position and intensity of the LMCT band for As<sup>III</sup>- $L^1$  as well as the lack of notable spectral changes between pH ~6.5 and 8.4 (see Figure S1) all point to a trithiolate coordination



of  $L^1$  to  $As^{III}$ . A pH-dependent series of spectra, recorded for the sample containing  $As^{III}$  and  $L^1$  in a 2:1 ratio, suggests a gradual decomposition of the  $AsL^1$  mono-complex above pH  $\sim 8.4$  (Figure S1). This process liberates the deprotonated free ligand, leading to the emergence of the  $n \rightarrow \sigma^*$  transition of the thiolate moieties, centered near 240 nm<sup>29,31,32</sup> (Figures S1 and S2). This is similar to what was observed with BAL<sup>31</sup> or DTE,<sup>32</sup> although only at higher pH (above pH  $\sim 10.0$ ), which might be a consequence of the higher affinity of  $As^{III}$  to the latter dithiolate molecules, which exhibit a strong chelate effect due to the formation of a five-membered ring involving the two As-bound thiolates, deferring the hydrolysis of the  $As^{III}$ –thiolate bonds (see below).

Gradual addition of arsenous acid to the solution of  $L^1$  shows the same saturation-like tendency in the recorded CD spectra as in the UV–vis data, i.e., the complexation process is completed only at a few-fold  $As^{III}$  excess over  $L^1$  (Figure 2). A

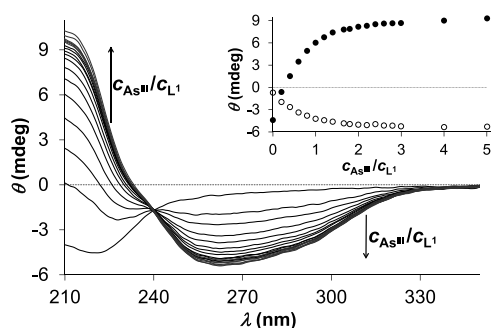


**Figure 2.** CD spectra of  $L^1$  recorded in a titration with arsenous acid at pH = 7.0 ( $c_{L^1} = 25 \mu M$  in phosphate buffer, 20 mM,  $I = 0.1 M$  NaCl). The inset shows the measured ellipticity traces at  $\lambda = 216$  nm (shaded circle) and at  $\lambda = 260$  nm (unshaded circle).

single isodichroic point around 240 nm, characteristic for the whole monitored  $c_{As^{III}}:c_{L^1}$  concentration ratio range, indicates that only one  $L^1$  complex is in equilibrium with the free ligand. CD spectroscopic data on systems of “colorless” metal ions and ligands with chirality centers near the metal ion binding groups<sup>16,17,19,35–37</sup> indicate that the positive and negative CD bands with intensity extrema near 210 and 260 nm, respectively, can be assigned to the LMCT transitions (vide supra). The optical activity of  $L^1$  is efficiently propagated from the  $\alpha$  carbon chirality centers toward  $As^{III}$  via the  $As^{III}$ –thiolate bonds. Similar to this, LMCT-related CD features also emerged in the UV region accompanying the coordination of the thiolate groups of  $L^{16}$  and  $L^{217,19}$  to  $Hg^{II}$  and  $Cu^I$ .

UV–vis and CD titrations performed for samples of  $As^{III}$ – $L^2$  (Figures S3 and S4) show similar trends to those for  $As^{III}$ – $L^1$ , characterizing a simple equilibrium between the free  $L^2$  and a trithiolate-coordinated complex  $AsL^2$ . However, the obtained absorbance and CD intensity vs  $As^{III}$ – $L^2$  concentration ratio profiles indicate a weaker  $As^{III}$  binding affinity of this bulkier compound that leads to a significant fraction of the ligand remaining unbound under the applied conditions even at high  $As^{III}$  excess.

**Results of ESI-MS Experiments.** ESI-MS studies confirm the presence of one major complex species of a 1:1  $As^{III}$ – $L^1$  ratio, which displays isotopic patterns corresponding to  $[L^1 - 4H^+ + As^{III}]^-$  and  $[L^1 - 3H^+ + As^{III} + Cl]^-$  compositions in the negative ion mode (Figure 3), which supports the binding of all the three thiolates to  $As^{III}$  in a monomeric species. ESI-

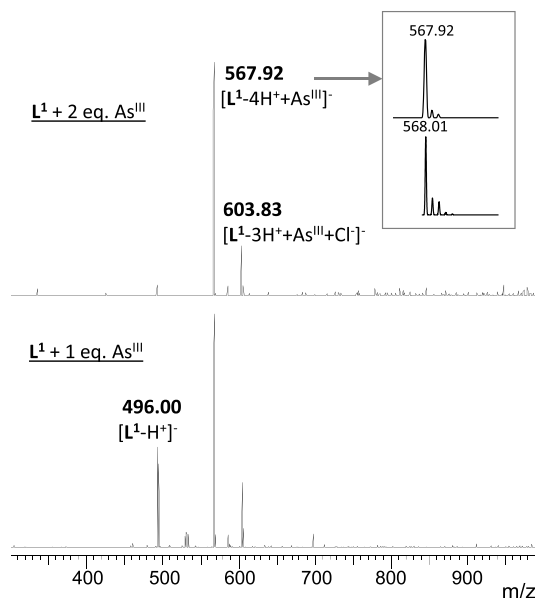


**Figure 3.** (–)ESI-MS spectra obtained for  $L^1$  with 1 eq. (down) and 2 eq. (top) of  $As^{III}$  at pH = 6.9 (ammonium acetate buffer 20 mM).

MS reflects the presence of monomeric species of  $L^2$ , too; however, signals of these adducts are very weak compared to those of the free ligand. Even in excess of  $As^{III}$ , for instance, for a 2:1  $As^{III}$ – $L$  ratio (Figure S5), where the spectrum acquired with  $L^1$  shows only the  $AsL^1$  complex (Figure 3 top), the  $AsL^2$  species is barely detected. This qualitatively implies that the binding of  $L^2$  to  $As^{III}$  is less efficient, which correlates well with the results of UV–vis- and CD-monitored titrations.

**Analysis of NMR Data.**  $^1H$  NMR data were also acquired for  $As^{III}$ – $L^1$  to gain insight into the structure of the trithiolate-bound species. Resonances of the free ligand gradually diminish, while new signals for the bound ligand, with significantly larger chemical shifts for the  $CH\alpha$  and  $CH_2\beta$  and altered splitting pattern of the NTA- $CH_2$  apical hydrogens (Figure 4 and Figure S6), emerge in parallel with the increasing  $As^{III}$ – $L^1$  concentration ratio (Figure 4). This

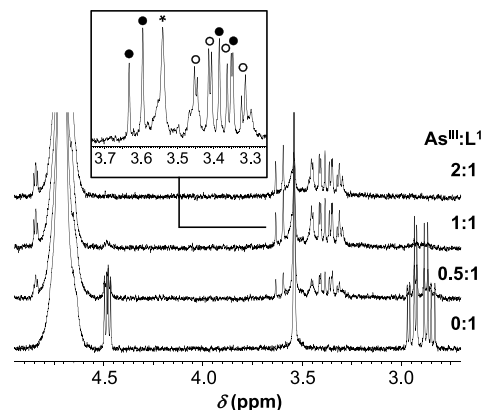


**Figure 4.** Selected region of the  $^1H$  NMR spectra of  $L^1$  in a titration by arsenous acid ( $c_{L^1} = 100 \mu M$  in  $D_2O$ , phosphate buffer, 20 mM, pH = 7.21). The framed section of a separately recorded spectrum displays resonances of the Cys  $CH_2\beta$  (unshaded circle) and the NTA- $CH_2$  apical hydrogen atoms (shaded circle) of the bound ligand; \* denotes residual resonances of the latter hydrogen atoms in the unbound ligand.

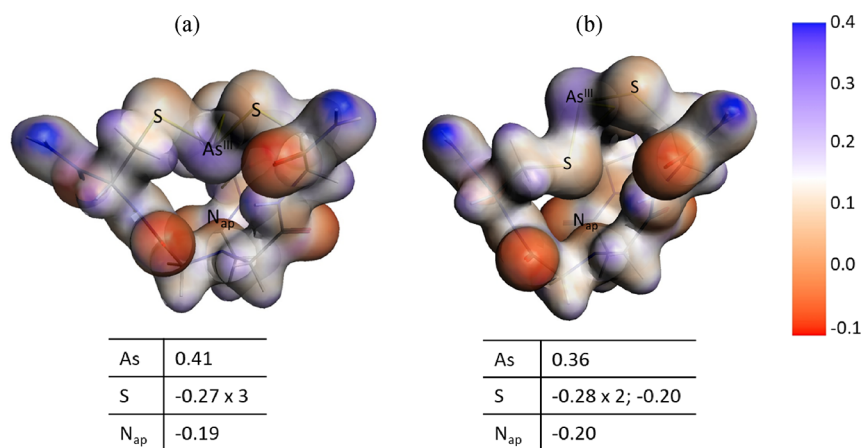


**Figure 5.** Electrostatic potential (in a.u.) projected on the electron density isosurface for  $\text{AsL}^1$  together with Mulliken charges (As, S, and  $\text{N}_{\text{ap}}$  atoms) on hel1 conformers: (a) *endo* and (b) *exo*.

indicates a slow ligand exchange at the NMR timescale in the  $\text{AsL}^1$  complex, which is in accordance with previous findings indicating a limited lability of the ligands bound in  $\text{As}^{\text{III}}$  complexes via two or three As–S bonds.<sup>30,31,38</sup> The splitting of the singlet of the NTA-CH<sub>2</sub> apical hydrogens of the unbound ligand into an AB spin system in  $\text{AsL}^1$  is a consequence of the blocked motion of the As-anchored ligand arms. In addition, one major resonance pattern is observed for the three NTA-CH<sub>2</sub>, the three CH $\alpha$ , and for the three CH<sub>2</sub> $\beta$  groups reflecting a C<sub>3</sub> symmetry of the complex. A couple of other low-intensity signals (e.g., at ca. 3.30 and 3.45 ppm; Figure 4 and Figure S6) may, however, indicate the presence of minor isomeric structures, too. These NMR data well support the findings of all other experiments and point to one major trithiolate-coordinated species displaying a highly symmetric orientation of the tripod arms around the semimetal center.

**Determination of the Stability of Species Formed under Neutral Conditions.** The binding affinity of  $\text{L}^1$  and  $\text{L}^2$  to arsenous acid was quantitatively assessed by evaluating UV–vis data (Figure 1 and Figure S3) in the wavelength range of 240–335 nm by using the PSEQUAD PC software.<sup>28</sup> The ligands are bound to arsenous acid in condensation reactions with no pH effect, as one water molecule per each forming As–S bond is released.<sup>31,32</sup> Accordingly, apparent stability constants for pH = 7.0 ( $\log K'$ ), characterizing the simple  $\text{As} + \text{L} \rightleftharpoons \text{AsL}$  equilibrium process with As denoting the free arsenous acid and L ( $\text{L}^1$  or  $\text{L}^2$ ) the unbound ligand in any protonation state, were calculated, as described previously.<sup>31</sup> The measured and calculated absorbance traces in Figure 1 (and in Figure S3), together with the relative fractions of the bound and unbound ligand, demonstrate that this simple model adequately describes the complexation processes:  $\log K'_{\text{AsL}^1} = 5.26 \pm 0.02$  and  $\log K'_{\text{AsL}^2} = 3.04 \pm 0.01$ , converted into  $K_{\text{d,AsL}^1} = 5.5 \mu\text{M}$  and  $K_{\text{d,AsL}^2} = 910 \mu\text{M}$  dissociation constants. Taking into account the similar basicities of the cysteine and penicillamine sidechain thiol groups,<sup>17</sup> the two orders of magnitude difference in the obtained stability values indicates a strong destabilizing effect of the methyl substituents in the D-Pen derivative.

**Computational Studies.** DFT molecular modeling was used to correlate the experimental data (especially those from NMR and the relative stabilities of the  $\text{AsL}^1$  and  $\text{AsL}^2$  species) with the most probable  $\text{As}^{\text{III}}$ -bound ligand structures. Previous theoretical (DFT) studies on various trigonal pyramidal  $\text{As}^{\text{III}}$

complexes showed that the conformation of the three  $\text{As}^{\text{III}}$ -bound moieties is not necessarily identical (*endo* or *exo*) in the energetically most favored structures.<sup>7,34</sup> Therefore, DFT geometry optimizations were launched from C<sub>3</sub> symmetric geometries of  $\text{AsL}^1$  and  $\text{AsL}^2$  with both possible helical configurations (named below hel1 and hel2) either from an all-*endo* (*endo,endo,endo*) or from an all-*exo* (*exo,exo,exo*) structure. The former yielded the most stable all-*endo* structures, whereas the latter relaxed systematically to an asymmetric mixed *endo,endo,exo* orientation of the S-CH<sub>2</sub> groups, higher in energy than the *endo* conformers (see Figures S7 and S8 and Tables S1 and S2). Scheme 1 displays the most stable all-*endo* and one *endo,endo,exo* conformers for  $\text{AsL}^1$ . The calculated As–S bond lengths (2.24–2.29 Å; Tables S3 and S4) are similar to those reported for low-molecular-weight  $\text{As}^{\text{III}}$  complexes,<sup>32,39</sup> the trigonal pyramidal  $\text{AsS}_3$  sites in three-helix bundles of oligopeptides,<sup>40,41</sup> or  $\text{As}^{\text{III}}$ -binding proteins.<sup>3,5,6,42,43</sup> Some H-bonding features are notably present inside one peptide arm and between two arms of the trigonal structure (Tables S3 and S4).

To confirm the all-*endo* to be the most stable structure, we simulated the UV–vis absorption spectra (Figure S9) and CD spectra (Figure S10) for  $\text{AsL}^1$  using time-dependent DFT approaches (see the Experimental Section). Whereas the absorption spectra do not allow to discriminate between conformers, the CD-simulated spectra are more significant. The *endo* hel1 CD spectrum clearly exhibits the same trend as the experimental one. Finally, some significant <sup>1</sup>H chemical shifts were calculated for  $\text{AsL}^1$  and are found to be similar to the experimental ones (Table S5). The same conformational ordering is obtained for the  $\text{AsL}^2$  species with an all-*endo* conformer as the most stable one (Table S2).

The reasons why the all-*endo* conformers are the most stable structures although the lone pairs of  $\text{As}^{\text{III}}$  and of the apical N atom point toward each other into the cavity may be found by careful examination of conformational as well as electronic properties of the  $\text{As}^{\text{III}}$  complexes. First, an isocontour plot of the electron density (Figure S11) shows that the lone pairs are not interacting. Additionally, previous DFT calculations on a small model  $\text{As}(\text{SMe})_3$  revealed that the most stable configurations were in a narrow energy range (2.2 kcal/mol), and particularly the all-*endo* conformer was only 1 kcal/mol higher than the most stable *endo,endo,exo* one.<sup>7</sup> This means that other environmental effects may control the final, most

favorable configuration as it was demonstrated in the various protein models chosen in this study. In our case, the relative energy ordering of the ligands alone, taken in the geometry of each of the conformers (Tables S1 and S2), follows the same order as that of the As<sup>III</sup> complexes, i.e., the all-*endo* ligand conformation is more stable than the *endo,endo,exo* one. Thus, the stabilization effects arising from the ligands themselves, such as intra- or inter-arm H-bonding, are not disrupted in the As<sup>III</sup>-bound species. Moreover, the actual interaction between As<sup>III</sup> and the apical nitrogen atom in both all-*endo* and *endo,endo,exo* conformers was examined based on atomic Mulliken charges and the electrostatic potential surface (Figure 5). The all-*endo* conformer provides a favorable electrostatic interaction with opposite charges on As and N, whereas the sulfur lone pairs point outside the cavity. Numerous structural combined to computational studies have described the nature of the pnictogen bond between As<sup>III</sup> trihalide species (mainly with F<sup>−</sup> or Cl<sup>−</sup>) and electron donor species such as N-, Se-, S-containing molecules or hexaalkylbenzene rings.<sup>13,44–47</sup> They all show donor–acceptor interactions, with As<sup>III</sup> being the electrophilic agent. Thanks to simple models, bond orientation preferences due to the so-called  $\sigma$ - or  $\pi$ -holes along the As lone pair have been described.<sup>13,44,46</sup> In a trigonal thiolate environment, the sulfur atom is expected to form a more covalent bond with As<sup>III</sup>, thus lowering its electrophilic character. Nevertheless, it has been shown by Vickaryous et al. that such a trigonal As(SR)<sub>3</sub> moiety is able to provide some stabilization interaction with aromatic rings,<sup>11</sup> as had been observed with As<sup>III</sup> trihalides.<sup>47,48</sup> The stabilization observed in the *endo,endo,endo* conformation of AsL<sup>1</sup> is thus in line with these previous observations. By contrast, the *endo,endo,exo* conformer displays a sulfur atom inside the cavity, which thus exhibits repulsive electrostatic interactions with the apical nitrogen. The absence of all-*exo* structures may be explained by the inability in such structures to balance the steric effects of sulfur lone pairs with the required As–S bond lengths and the chelating organization of the tripodal ligand, as already noticed by Zampella et al.<sup>7</sup> Indeed, in this study, the authors also pointed out that the most favored conformations of As(SMe)<sub>3</sub> moieties are the *endo,endo,exo* and all-*endo* isomers differing only by 1 kcal/mol in energy. Interestingly, we observe that ligands L<sup>1</sup> and L<sup>2</sup> give energetically favorable conformations to accommodate the all-*endo* isomer. This observation evidences the good adjustment of the tripodal pseudopeptide ligands proposed in this study to stabilize the As<sup>III</sup> coordination environment.

## CONCLUSIONS

In this work, we demonstrated that the NTA-based tripodal ligands bearing three Cys or D-Pen arms exclusively stabilize the AsS<sub>3</sub> coordination environment of As<sup>III</sup>. The stability of the species formed with the sterically less restricted NTA(Cys-NH<sub>2</sub>)<sub>3</sub> ligand is in the range determined (by a different method and under somewhat different conditions) for As<sup>III</sup>-oligopeptide complexes displaying two or three bound cysteines, with a slight possible extra stabilizing effect of the third coordinating sulfur.<sup>49</sup> A combination of experimental and theoretical studies pointed to an all-*endo* conformer as the favored structure for the As<sup>III</sup> complexes of both ligands, originating from stabilizing electrostatic interactions between the lone pair of As and the apical nitrogen atom.

The AsS<sub>3</sub> coordination sphere imposed by the two biomimetic ligands is reminiscent of As<sup>III</sup>-bound protein or

peptide species, with a preference for the all-*endo* conformer, which mimics the As<sup>III</sup> coordination environment in the three cysteine-bound As<sup>III</sup> semimetal sites in metalloproteins. Indeed, although the crystal structures found in the literature for the As<sup>III</sup> complexes of bioligands, i.e., a three-stranded coiled-coil peptide,<sup>50</sup> the metalloregulators CgArsR<sup>6</sup> and AfArsR,<sup>6</sup> or the ArsM protein,<sup>5</sup> reflect some variability, all of these trithiolate-coordinated semimetal centers display at least two *endo*-type S-CH<sub>2</sub> carbon atoms around As<sup>III</sup>.

## ASSOCIATED CONTENT

### Supporting Information

The Supporting Information is available free of charge at <https://pubs.acs.org/doi/10.1021/acs.inorgchem.3c00563>.

Tables of DFT-optimized parameters, figures of UV–vis, ESI-MS, and NMR spectra as well as of DFT-optimized structures (PDF)

## AUTHOR INFORMATION

### Corresponding Authors

Pascale Delangle – CEA, CNRS, Grenoble INP, IRIG, SyMMES, Université Grenoble Alpes, Grenoble 38000, France; [orcid.org/0000-0002-8546-9080](https://orcid.org/0000-0002-8546-9080); Email: [pascale.delangle@cea.fr](mailto:pascale.delangle@cea.fr); Fax: (+33) 438785090

Attila Jancsó – Department of Inorganic and Analytical Chemistry, University of Szeged, Szeged H-6720, Hungary; [orcid.org/0000-0003-2362-0758](https://orcid.org/0000-0003-2362-0758); Email: [jancso@chem.u-szeged.hu](mailto:jancso@chem.u-szeged.hu); Fax: (+36) 62544340

### Authors

Levente I. Szekeres – Department of Inorganic and Analytical Chemistry, University of Szeged, Szeged H-6720, Hungary; Present Address: Present address of Levente Szekeres: Protein Bioinformatics Research Group, Institute of Enzymology, Research Centre for Natural Sciences, Magyar Tudósok körútja 2, Budapest H-1117, Hungary (L.I.S.)

Pascale Maldivi – CEA, CNRS, Grenoble INP, IRIG, SyMMES, Université Grenoble Alpes, Grenoble 38000, France; [orcid.org/0000-0003-2008-1090](https://orcid.org/0000-0003-2008-1090)

Colette Lebrun – CEA, CNRS, Grenoble INP, IRIG, SyMMES, Université Grenoble Alpes, Grenoble 38000, France

Christelle Gateau – CEA, CNRS, Grenoble INP, IRIG, SyMMES, Université Grenoble Alpes, Grenoble 38000, France

Edit Mesterházy – Department of Inorganic and Analytical Chemistry, University of Szeged, Szeged H-6720, Hungary; CEA, CNRS, Grenoble INP, IRIG, SyMMES, Université Grenoble Alpes, Grenoble 38000, France

Complete contact information is available at:

<https://pubs.acs.org/10.1021/acs.inorgchem.3c00563>

### Author Contributions

The manuscript was written through contributions of all authors. All authors have given approval to the final version of the manuscript.

### Notes

The authors declare no competing financial interest.



## ■ ACKNOWLEDGMENTS

The authors gratefully acknowledge research support of this work by the French National Agency for Research in the framework of the “Investissements d’avenir” Program (ANR-15-IDEX-02), the Labex ARCAN (ANR-11-LABX-003), and the CBH-EUR-GS (ANR-17-EURE-0003) and also Campus France and CNRS for funding the stays at SyMMES in France of L.I.S. and A.J., as an invited student and an invited researcher, respectively.

## ■ REFERENCES

- (1) Wright, J. G.; Tsang, H. T.; Pennerhahn, J. E.; O'Halloran, T. V. Coordination Chemistry of the Hg-MerR Metalloregulatory Protein - Evidence for a Novel Tridentate Hg-Cysteine Receptor-Site. *J. Am. Chem. Soc.* **1990**, *112*, 2434–2435.
- (2) Calderone, V.; Dolderer, B.; Hartmann, H. J.; Echner, H.; Luchinat, C.; Del Bianco, C.; Mangani, S.; Weser, U. The crystal structure of yeast copper thionein: The solution of a long-lasting enigma. *Proc. Natl. Acad. Sci. U. S. A.* **2005**, *102*, 51–56.
- (3) Ye, J.; Ajees, A. A.; Yang, J.; Rosen, B. P. The 1.4 Å Crystal Structure of the ArsD Arsenic Metallochaperone Provides Insights into Its Interaction with the ArsA ATPase. *Biochemistry* **2010**, *49*, 5206–5212.
- (4) Shen, S.; Li, X.-F.; Cullen, W. R.; Weinfeld, M.; Le, X. C. Arsenic Binding to Proteins. *Chem. Rev.* **2013**, *113*, 7769–7792.
- (5) Packianathan, C.; Kandavelu, P.; Rosen, B. P. The Structure of an As(III) S-Adenosylmethionine Methyltransferase with 3-Coordinate Bound As(III) Depicts the First Step in Catalysis. *Biochemistry* **2018**, *57*, 4083–4092.
- (6) Prabakaran, C.; Kandavelu, P.; Packianathan, C.; Rosen, B. P.; Thiagarajana, S. Structures of two ArsR As(III)-responsive transcriptional repressors: Implications for the mechanism of derepression. *J. Struct. Biol.* **2019**, *207*, 209–217.
- (7) Zampella, G.; Neupane, K. P.; De Gioia, L.; Pecoraro, V. L. The Importance of Stereochemically Active Lone Pairs For Influencing Pb<sup>II</sup> and As<sup>III</sup> Protein Binding. *Chem. – Eur. J.* **2012**, *18*, 2040–2050.
- (8) Carter, T. G.; Healey, E. R.; Pitt, M. A.; Johnson, D. W. Secondary Bonding Interactions Observed in Two Arsenic Thiolate Complexes. *Inorg. Chem.* **2005**, *44*, 9634–9636.
- (9) Carter, T. G.; Vickaryous, W. J.; Cangelosi, V. M.; Johnson, D. W. Supramolecular Arsenic Coordination Chemistry. *Comments Inorg. Chem.* **2007**, *28*, 97–122.
- (10) Cangelosi, V. M.; Zakharov, L. N.; Crossland, J. L.; Franklin, B. C.; Johnson, D. W. A Surprising “Folded-In” Conformation of a Self-Assembled Arsenic-Thiolate Macrocycle. *Cryst. Growth Des.* **2010**, *10*, 1471–1473.
- (11) Vickaryous, W. J.; Herges, R.; Johnson, D. W. Arsenic- $\pi$  Interactions Stabilize a Self-Assembled As<sub>2</sub>L<sub>3</sub> Supramolecular Complex. *Angew. Chem., Int. Ed.* **2004**, *43*, 5831–5833.
- (12) Pitt, M. A.; Zakharov, L. N.; Vanka, K.; Thompson, W. H.; Laird, B. B.; Johnson, D. W. Multiple weak supramolecular interactions stabilize a surprisingly twisted As<sub>2</sub>L<sub>3</sub> assembly. *Chem. Commun.* **2008**, 3936–3938.
- (13) Bauzá, A.; Quiñonero, D.; Deyá, P. M.; Frontera, A. Pnicogen- $\pi$  complexes: theoretical study and biological implications. *Phys. Chem. Chem. Phys.* **2012**, *14*, 14061–14066.
- (14) Murray, J. S.; Lane, P.; Politzer, P. A Predicted New Type of Directional Noncovalent Interaction. *Int. J. Quant. Chem.* **2007**, *107*, 2286–2292.
- (15) Murray, J. S.; Lane, P.; Clark, T.; Riley, K. E.; Politzer, P.  $\sigma$ -Holes,  $\pi$ -holes and electrostatically-driven interactions. *J. Mol. Model.* **2012**, *18*, 541–548.
- (16) Pujol, A. M.; Gateau, C.; Lebrun, C.; Delangle, P. A Series of Tripodal Cysteine Derivatives as Water-Soluble Chelators that are Highly Selective for Copper(I). *Chem. – Eur. J.* **2011**, *17*, 4418–4428.
- (17) Jullien, A.-S.; Gateau, C.; Lebrun, C.; Kieffer, I.; Testemale, D.; Delangle, P. D-Penicillamine Tripodal Derivatives as Efficient Copper(I) Chelators. *Inorg. Chem.* **2014**, *53*, 5229–5239.
- (18) Pujol, A. M.; Lebrun, C.; Gateau, C.; Manceau, A.; Delangle, P. Mercury-Sequestering Pseudopeptides with a Triscysteine Environment in Water. *Eur. J. Inorg. Chem.* **2012**, 3835–3843.
- (19) Jullien, A. S.; Gateau, C.; Lebrun, C.; Delangle, P. Mercury Complexes with Tripodal Pseudopeptides Derived from D-Penicillamine Favour a HgS<sub>3</sub> Coordination. *Eur. J. Inorg. Chem.* **2015**, 3674–3680.
- (20) Ellman, G. L. Tissue sulfhydryl groups. *Arch. Biochem. Biophys.* **1959**, *82*, 70–77.
- (21) Riddles, P. W.; Blakeley, R. L.; Zerner, B. Reassessment of Ellman's reagent. *Methods Enzymol.* **1983**, *91*, 49–60.
- (22) Neese, F. The ORCA Program System. *WIREs Comput. Mol. Sci.* **2012**, *2*, 73–78.
- (23) Neese, F. Software Update: The ORCA Program System, Version 4.0. *WIREs Comput. Mol. Sci.* **2018**, *8*, No. e1327.
- (24) Neese, F.; Wennmohs, F.; Becker, U.; Riplinger, C. The ORCA Quantum Chemistry Program Package. *J. Chem. Phys.* **2020**, *152*, No. 224108.
- (25) Stoychev, G. L.; Auer, A. A.; Izsák, R.; Neese, F. Self-Consistent Field Calculation of Nuclear Magnetic Resonance Chemical Shielding Constants Using Gauge-Including Atomic Orbitals and Approximate Two-Electron Integrals. *J. Chem. Theory Comput.* **2018**, *14*, 619–637.
- (26) Chemcraft - graphical software for visualization of quantum chemistry computations. <https://www.chemcraftprog.com>.
- (27) te Velde, G.; Bickelhaupt, F. M.; Baerends, E. J.; Fonseca Guerra, C.; van Gisbergen, S. J. A.; Snijders, J. G.; Ziegler, T. Chemistry with ADF. *J. Comput. Chem.* **2001**, *22*, 931–967.
- (28) Zekany, I.; Nagypal, I.; Peintler, G. PSEQUAD for chemical equilibria. Technical Software Distributors, Baltimore, MD, 1991.
- (29) Rey, N. A.; Howarth, O. W.; Pereira-Maia, E. C. J. Equilibrium characterization of the As(III)-cysteine and the As(III)-glutathione systems in aqueous solution. *J. Inorg. Biochem.* **2004**, *98*, 1151–1159.
- (30) Spuches, A. M.; Kruszyna, H. G.; Rich, A. M.; Wilcox, D. E. Thermodynamics of the As(III)-Thiol Interaction: Arsenite and Monomethylarsenite Complexes with Glutathione, Dihydrolipoic Acid, and Other Thiol Ligands. *Inorg. Chem.* **2005**, *44*, 2964–2972.
- (31) Szekeres, L. I.; Gyurcsik, B.; Kiss, T.; Kele, Z.; Jancsó, A. Interaction of Arsenous Acid with the Dithiol-Type Chelator British Anti-Lewisite (BAL): Structure and Stability of Species Formed in an Unexpectedly Complex System. *Inorg. Chem.* **2018**, *57*, 7191–7200.
- (32) Kolozsi, A.; Lakatos, A.; Galbács, G.; Madsen, A. Ø.; Larsen, E.; Gyurcsik, B. A pH-Metric, UV, NMR, and X-ray Crystallographic Study on Arsenous Acid Reacting with Dithioerythritol. *Inorg. Chem.* **2008**, *47*, 3832–3840.
- (33) Ezech, V. C.; Patra, A. K.; Harrop, T. C. Four-Coordinate As<sup>III</sup>-N,S Complexes: Synthesis, Structure, Properties, and Biological Relevance. *Inorg. Chem.* **2010**, *49*, 2586–2588.
- (34) Garla, R.; Kaur, N.; Bansal, M. P.; Garg, M. L.; Mohanty, B. P. Quantum mechanical treatment of As<sup>3+</sup>-thiol model compounds: implication for the core structure of As(III)-metallothionein. *J. Mol. Model.* **2017**, *23*, 78.
- (35) Pires, S.; Habjanič, J.; Sezer, M.; Soares, C. M.; Hemmingsen, L.; Olga Iranzo, O. Design of a Peptidic Turn with High Affinity for Hg<sup>II</sup>. *Inorg. Chem.* **2012**, *51*, 11339–11348.
- (36) Mesterházy, E.; Lebrun, C.; Crouzy, S.; Jancsó, A.; Delangle, P. Short oligopeptides with three cysteine residues as models of sulphur-rich Cu(I)- and Hg(II)-binding sites in proteins. *Metallomics* **2018**, *10*, 1232–1244.
- (37) Pantcheva, I.; Nedzhib, A.; Antonov, L.; Gyurcsik, B.; Dorkov, P. New insights into coordination chemistry of Monensin A towards divalent metal ions. *Inorg. Chim. Acta* **2020**, *505*, No. 119481.
- (38) Kitchin, K. T.; Wallace, K. Dissociation of Arsenite-Peptide Complexes: Triphasic Nature, Rate Constants, Half-lives, and Biological Importance. *J. Biochem. Mol. Toxicol.* **2006**, *20*, 48–56.

(39) Cruse, W. B. T.; James, M. N. G. The Crystal Structure of the Arsenite Complex of Dithiothreitol. *Acta Crystallogr., Sect. B: Struct. Crystallogr. Cryst. Chem.* **1972**, B28, 1325–1331.

(40) Farrer, B. T.; McClure, C. P.; Penner-Hahn, J. E.; Pecoraro, V. L. Arsenic(III)-Cysteine Interactions Stabilize Three-Helix Bundles in Aqueous Solution. *Inorg. Chem.* **2000**, 39, 5422–5423.

(41) Matzapetakis, M.; Farrer, B. T.; Weng, T.-C.; Hemmingsen, L.; Penner-Hahn, J. E.; Pecoraro, V. L. Comparison of the Binding of Cadmium(II), Mercury(II), and Arsenic(III) to the de Novo Designed Peptides TRI L12C and TRI L16C. *J. Am. Chem. Soc.* **2002**, 124, 8042–8054.

(42) Qin, J.; Fu, H.-L.; Ye, J.; Bencze, K. Z.; Stemmler, T. L.; Rawlings, D. E.; Rosen, B. P. Convergent Evolution of a New Arsenic Binding Site in the ArsR/SmtB Family of Metalloregulators. *J. Biol. Chem.* **2007**, 282, 34346–34355.

(43) Ordóñez, E.; Thiagarajan, S.; Cook, J. D.; Stemmler, T. L.; Gil, J. A.; Mateos, L. M.; Rosen, B. P. Evolution of Metal(loid) Binding Sites in Transcriptional Regulators. *J. Biol. Chem.* **2008**, 283, 25706–25714.

(44) Varadwaj, A.; Varadwaj, P. R.; Marques, H. M.; Yamashita, K. The Pnictogen Bond: The Covalently Bound Arsenic Atom in Molecular Entities in Crystals as a Pnictogen Bond Donor. *Molecules* **2022**, 27, 3421.

(45) Bauzá, A.; Quiñero, D.; Deyà, P. M.; Frontera, A. Halogen Bonding Versus Chalcogen and Pnicogen Bonding: a Combined Cambridge Structural Database and Theoretical Study. *CrystEngComm* **2013**, 15, 3137–3144.

(46) Bauzá, A.; Alkorta, I.; Frontera, A.; Elguero, J. On the Reliability of Pure and Hybrid DFT Methods for the Evaluation of Halogen, Chalcogen, and Pnicogen Bonds Involving Anionic and Neutral Electron Donors. *J. Chem. Theory Comput.* **2013**, 9, 5201–5210.

(47) Probst, T.; Steigelmann, O.; Riede, J.; Schmidbaur, H. Arsen(III)-, Antimon(III)- und Bismuth(III)-halogenid-Komplexe des [2.2.2]Paracyclophans: Vom lockeren van-der-Waals-Addukt zu Stark Gerichteten  $\pi$ -Komplexen mit Zwei- und Dreifacher Externer  $\eta^6$ -Koordination. *Chem. Ber.* **1991**, 124, 1089–1093.

(48) Schmidbaur, H.; Bublak, W.; Huber, B.; Müller, G. Arene Adducts with Weak Interactions: Hexaethylbenzene-bis-(tribromoarsane). *Angew. Chem., Int. Ed. Engl.* **1987**, 26, 234–236.

(49) Kitchin, K. T.; Wallace, K. Arsenite Binding to Synthetic Peptides Based on the Zn Finger Region and the Estrogen Binding Region of the Human Estrogen Receptor- $\alpha$ . *Toxicol. Appl. Pharmacol.* **2005**, 206, 66–72.

(50) Touw, D. S.; Nordman, C. E.; Stuckey, J. A.; Pecoraro, V. L. Identifying Important Structural Characteristics of Arsenic Resistance Proteins by Using Designed Three-Stranded Coiled Coils. *Proc. Natl. Acad. Sci.* **2007**, 104, 11969–11974.

## Recommended by ACS

### Increased Efficiency of a Functional SOD Mimic Achieved with Pyridine Modification on a Pycen-Based Copper(II) Complex

Magy A. Mekhail, Kayla N. Green, *et al.*

MARCH 30, 2023  
INORGANIC CHEMISTRY

READ 

### Theoretical Understanding of Reactions of Rhenium and Ruthenium Tris(thiolate) Complexes with Unsaturated Hydrocarbons: Noninnocent Nature of the Ligand, Mecha...

Jia Guan, Hao Tang, *et al.*

JANUARY 31, 2023  
INORGANIC CHEMISTRY

READ 

### N,N-Alkylation Clarifies the Role of N- and O-Protonated Intermediates in Cyclen-Based $^{64}\text{Cu}$ Radiopharmaceuticals

Alexander M. Brown, Jerome R. Robinson, *et al.*

DECEMBER 09, 2022  
INORGANIC CHEMISTRY

READ 

### Solvent Extraction and Conformation Rigidity: Actinide(IV) and Actinide(VI) Come Together

Nataliya E. Borisova, Mariia V. Evsiunina, *et al.*

DECEMBER 14, 2022  
INORGANIC CHEMISTRY

READ 

Get More Suggestions >